PCCP

Stochastic description of precipitate pattern formation in an electric field

István Lagzi[a] and Ferenc Izsák[b]

[a] *Department of Physical Chemistry, Eötvös University (ELTE), H-1518, Budapest, P.O. Box 32, Hungary. E-mail: lagzi@vuk.chem.elte.hu; Fax: 36 1209 0602; Tel: 36 1209 0555*
[b] *Department of Applied Analysis, Eötvös University (ELTE), H-1518, Budapest, P.O. Box 120, Hungary. E-mail: bizsu@cs.elte.hu; Fax: 36 1381 2158; Tel: 36 1381 2157*

Received 22nd May 2003, Accepted 19th August 2003
First published as an Advance Article on the web 5th September 2003

Evolution of Liesegang patterns in an external electric field was studied numerically using a discrete stochastic model and by real experiments. In the stochastic model the diffusion was described by a Brownian random walk of discrete particles. The precipitation reaction was regarded to be a stochastic process as well, and its description was based on Ostwald's supersaturation theory. Our real experiments and the results of this stochastic approach have shown a good agreement. On the basis of our results we have proposed an extended form of the width law, which takes into account the effect of constant electric field.

Introduction

The first rhythmic precipitation patterns were observed and studied by R. E. Liesegang in 1896.[1] When an electrolyte (called the outer electrolyte) diffuses into a gel matrix, which contains another electrolyte (called the inner electrolyte), the precipitation reaction between them produces a quasiperiodic precipitate distribution.

Several models and theories have been developed in order to describe this so-called Liesegang phenomenon[2–9] which has four empirical regularities (the spacing law,[10] the time law,[11] the width law[12–14] and the Matalon–Packter law[15,16]). According to the spacing law X_{n+1}/X_n approaches a constant P_{sp} for large enough values of n, where X_n and X_{n+1} are the positions of the nth and $(n+1)$th bands measured from the junction point of the two electrolytes and P_{sp} is the so-called spacing coefficient. The time law makes connection between the time elapsed until the formation of the nth zone (t_n), and its position: $X_n = a_o t_n^{1/2} + c_o$, where a_o, c_o are constants. This is an immediate consequence of the diffusion process. According to the width law $w_n \propto X_n^{\alpha}$, where w_n is the width of the nth band. Experimental results[13] and a deterministic simulation[17] suggest that the exponent α is close to *one*. However, the cellular automata model of Chopard *et al.* resulted in α values that fall into the range 0.5–0.6[18,19] and similar values have been found by Izsák and Lagzi[20] using a different stochastic approach.

Most of the precipitates in Liesegang experiments are formed by ions, therefore an electric field is expected to have significant effect on the spatiotemporal evolution of these patterns.

The first such experiments were carried out in the twenties of the last century.[21–23] Recently, Sharbaugh and Sharbaugh[24] performed such experiments with the $CuSO_4/Na_2CrO_4$ system in silica gel. Das *et al.* performed similar studies in 1D[25] and 2D[26] with the $KI/HgCl_2$ system in agar gel. Sultan and Halabieh,[27] and Sultan[28] applied the $NH_4OH/CoCl_2$ system in gelatin gel, while Sultan and Panjarian[29] studied the $NaOH/Cr(NO_3)_3$ reaction in PVA gel in 2D. Finally Lagzi has recently studied the influence of an electric field on the $AgNO_3/K_2Cr_2O_7$ system in gelatine.[30]

The basic consequence of this earlier work was that the velocity of propagation of the reaction front can be characterized by the following function $X_n = at_n^{1/2} + bt_n + c$, where a, b and c are constants. At the same time the spacing coefficient P_{sp} decreases with field strength.[30]

In a recent paper an extended form of the deterministic model proposed by Büki *et al.*[5] has been developed in accordance with external field effects. This numerical model was based on Ostwald's supersaturation theory,[31] and reproduced successfully the experimentally observed time dependence and variation of spacing coefficient with the field strength.

Al-Ghoul and Sultan[32] studied recently the redissolution of precipitate in an electric field, however they used the model of Polezhaev and Müller[4] as a basis.

Until now, neither experimental nor numerical studies were devoted to the investigation of the width law in an electric field.

In the "classical" deterministic models of Liesegang patterning the stochastic effects like fluctuations in the concentration distributions are generally ignored. At the same time there are some phenomena that are usually attributed to the existence of such randomizing impacts.[33,34] In the recent literature one can find only a few mathematical models that incorporate such stochastic effects,[18,19,20,35] but none of them takes into account the effect of an external electric field.

In the present paper we provide a stochastic numerical approach to describe such a situation. In order to validate the model we have performed some real experiments as well, studying the effect of the electric field on the width law.

Experimental

The gel was prepared by adding 9.50 g gelatine (Reanal) to 250 mL of 0.0036 M $K_2Cr_2O_7$ (Reanal) solution. The mixture was heated to 65–75 °C and stirred continuously. After complete dissolution of the gelatine the solution was poured into glass tubes of diameter 6 mm and length 19.0 cm. The tubes were then allowed to cool to room temperature (23 ± 2 °C). All experiments were carried out without thermostatic control.

 DOI: 10.1039/b305728c

The tubes were placed horizontally and the right and left ends of the gel column were brought into contact with a solution of $K_2Cr_2O_7$ (0.0036 M) and a solution of $AgNO_3$ (Reanal, 5.70 w/w %). Into these solutions silver and platinum electrodes were placed, and were connected to a power supply (Elektroflex EF 1307) by which we have maintained potentiostatic polarization.

The formation of precipitate bands was monitored by a CCD camera (Panasonic WV-BP310/G), connected to a computer-controlled imaging system. The tubes were properly illuminated in order that the video system could record the light reflected from the colloid particles.[30] The electric field strength (**E**) was varied between -12 V m^{-1} and 18 V m^{-1}.

The stochastic model

The stochastic model incorporates a simple chemical reaction between two electrolytes

$$A^+(aq) + B^-(aq) \rightarrow AB(s),$$

where $A^+(aq)$ and $B^-(aq)$ are the ionic species and AB(s) is the precipitate. The space is discretized into N small segments ("boxes"), which means that the overall state of the system can always be described by three state vectors $M_A(t)$, $M_B(t)$ and $M_{AB}(t)$, of length N. The ith component of a vector contains the number of the corresponding particles at the given segment at time t.

An operator $\boldsymbol{F}$ was defined in order to describe the spatio-temporal evolution of the pattern over a time step h. This operator must account for the joint effect of diffusion, ionic migration and precipitation reaction. Formally, these can be described by the following equation:

$$\boldsymbol{F}(M_A[i](t),\ M_B[i](t),\ M_{AB}[i](t)) = (M_A[i](t+h),\ M_B[i](t+h),\ M_{AB}[i](t+h)).$$

In stochastic models diffusion of the electrolytes is usually described by a discrete Brownian motion. However, we wanted to handle diffusion and migration of ions as a whole, therefore we have applied a shifted normal distribution function $N(m, \sigma)$. Here m corresponds to the advection, while σ describes the extent of the diffusion.

First, we describe the case which is free of ionic migration. (In the following we will apply the same discrete approach and the same notions as in our previous paper[20].) In such a discrete description we can treat only discrete positions and transitions. At the same time, movement of particles in an ensemble is spatially continuous, which means that we have to apply a mapping between the continuous distribution of displacements and the discrete description.

In the discrete model displacements of particles between the -0.5 and 0.5 neighborhood of their actual position correspond to "step = 0", that is, they will rest at the same segment. Similarly, particles with displacements between -0.5 and -1.5 are mapped to the segment to the left of the actual one ("step = -1"), while those between $+0.5$ and $+1.5$ will go to the position to the right of the actual position.

In our model we have allowed five steps: -2, -1, 0, 1, 2. Choosing the standard normal distribution ($N(0, 1)$) with the density function

$$\Phi(x) = \frac{1}{\sqrt{2\pi}} e^{-\frac{x^2}{2}}$$

we obtain the following transition probabilities:

$$p_2 = P(\text{step} = 2) = p_{-2} = P(\text{step} = -2) = \int_{-\infty}^{-1.5} \Phi(x)\mathrm{d}x \approx 0.0668,$$

$$p_1 = P(\text{step} = 1) = p_{-1} = P(\text{step} = -1) = \int_{-1.5}^{-0.5} \Phi(x)\mathrm{d}x \approx 0.2417,$$

$$p_0 = P(\text{step} = 0) = \int_{-0.5}^{0.5} \Phi(x)\mathrm{d}x \approx 0.383.$$

Generally, we denote with $p[i][j]$ the probability that a particle moves from the ith segment to the jth one.

We model the effect of the homogeneous electric field by modifying these transition probabilities (P into P_ε) as follows. In the real experiments the transport number of the outer electrolyte is much higher than that of the inner one. Therefore it has been supposed that the external field influences only the transport of the electrolyte coming from outside. This means that we had to modify only the transition probabilities of A particles.

If the electric field promotes the movement of the reaction front ("positive field") we push every A particle to the right with probability ε_+ and leave it in its original position with probability $1 - \varepsilon_+$. ε_+ is a measure of the electric field strength. In smmary, the transition probabilities of A particles are given by the following equations:

$$P_{\varepsilon_+}(\text{step} = 1) = P(\text{step} = 0)\varepsilon_+ + P(\text{step} = 1)(1 - \varepsilon_+) = p_0\varepsilon_+ + p_1(1 - \varepsilon_+),$$

$$P_{\varepsilon_+}(\text{step} = 0) = p_{-1}\varepsilon_+ + p_0(1 - \varepsilon_+),$$
$$P_{\varepsilon_+}(\text{step} = -1) = p_{-2}\varepsilon_+ + p_{-1}(1 - \varepsilon_+),$$
$$P_{\varepsilon_+}(\text{step} = -2) = p_{-2}(1 - \varepsilon_+),$$
$$P_{\varepsilon_+}(\text{step} = 2) = p_1\varepsilon_+ + p_2\,.$$

The case $\varepsilon_+ = 0$ corresponds to the absence of an electric field.

Similarly, if the electric field retards the diffusion of the outer electrolyte A ("negative field"), we modify the transition probabilities as follows:

$$P_{\varepsilon_-}(\text{step} = 1) = p_2\varepsilon_- + p_1(1 - \varepsilon_-),$$
$$P_{\varepsilon_-}(\text{step} = 0) = p_1\varepsilon_- + p_0(1 - \varepsilon_-),$$
$$P_{\varepsilon_-}(\text{step} = -1) = p_0\varepsilon_- + p_{-1}(1 - \varepsilon_-),$$
$$P_{\varepsilon_-}(\text{step} = -2) = p_{-1}\varepsilon_- + p_{-2}\,,$$
$$P_{\varepsilon_-}(\text{step} = 2) = p_2(1 - \varepsilon_-),$$

where ε_- again characterizes the electric field strength. We assumed that the precipitate does not diffuse. The precipitation reaction was modeled by Ostwald's supersaturation theory[31] the basic idea of which is that precipitation can take place only if the local concentration product of the electrolytes reaches a certain threshold (nucleation product). However, after the formation of the first crystals the product of the reaction promotes the further process and the mentioned threshold value falls back to the thermodynamic solubility product.[5]

In our discrete model, we treat particle numbers instead of concentrations. During the calculation of their actual values we have taken into account all the particles, that reside or go through a given segment. These summed up particle numbers are denoted by $\mathrm{SUM_A}[i](t)$ and $\mathrm{SUM_B}[i](t)$. The originality of our approach lies in that, while in the "classical" approach only "point concentrations" ($M_A[i](t)$ and $M_B[i](t)$) are used to calculate the reaction term, we use these generalized concentrations. This generalization makes it possible to take into account some stochastic effects.

In the simulations we calculated the reaction term by the following algorithm. If $M_{AB}[i](t)$ was 0 (there is no precipitate at the ith segment), a deterministic approach would result in the following amount of precipitated material:

$$\Delta[i](t) = \delta[i](t)\Theta(\mathrm{SUM_A}[i](t)\mathrm{SUM_B}[i](t) - K).$$

At the same time if $M_{AB}[i] \neq 0$, then

$$\Delta[i](t) = \delta[i](t)\Theta(\mathrm{SUM_A}[i](t)\mathrm{SUM_B}[i](t) - L),$$

where L is the solubility product, K is the nucleation product, Θ is the Heaviside step function, and $\delta[i](t)$ denotes the precipitated amount. For an AB type precipitate this latter can be calculated based on the following algebraic equation:[5,36]

$$\begin{aligned}\delta[i](t) = 0.5((&\mathrm{SUM_A}[i](t) + \mathrm{SUM_B}[i](t)) \\ &- [(\mathrm{SUM_A}[i](t) + \mathrm{SUM_B}[i](t))^2 \\ &- 4(\mathrm{SUM_A}[i](t)\mathrm{SUM_B}[i](t) - L)]^{\frac{1}{2}}).\end{aligned}$$

Formation of the precipitate stops wherever $M_{AB}[i]$ reaches a maximal value ($M_{AB,max}$).

The reaction probability – the probability that a given A particle transforms into precipitate – is given by the ratio $q_A[i](t) = \Delta[i](t)/\mathrm{SUM_A}[i](t)$. Certainly B particles have a similar value q_B. Not all particles (A and B) that were taken into account during the calculation of $\mathrm{SUM_A}[i](t)$ and $\mathrm{SUM_B}[i](t)$ will be transformed into precipitate in one time step. The probability of this event can be calculated as $1 - q_A[i](t)$. According to the precipitation reaction we have to modify the transition probabilities. If $j \leq i \leq k$ then the probability that a given particle A or B, which moves from the jth segment to kth one, does not transform into precipitate can be calculated as the product

$$\prod_{j\leq i\leq k}(1 - q_A[i](t)) \quad \text{and} \quad \prod_{j\leq i\leq k}(1 - q_B[i](t)).$$

In this way the modified transition probabilities ($p^*_\varepsilon[j][k]$ and $p^*[j][k]$) will be

$$p^*_\varepsilon[j][k] = p_\varepsilon[j][k]\prod_{j\leq i\leq k}(1 - q_A[i](t)),$$

$$p^*[j][k] = p[j][k]\prod_{j\leq i\leq k}(1 - q_B[i](t)).$$

Practically, for A particles in the jth segment we created discrete intervals in [0,1] of length $p^*_\varepsilon[j][1]$, $p^*_\varepsilon[j][2]$,...$p^*_\varepsilon[j][N]$ and for each of the particles a random number RND in [0,1]. If this fell into the interval corresponding to $p^*_\varepsilon[j][k]$ then we pushed the particle into the kth segment. Anyway, if none of the intervals covered RND, we transformed the particle into precipitate. We proceed similarly for B particles.

The following parameter set was used in the simulations: $K = 1400$, $L = 300$, $M_{AB,max} = 1000$ and $N = 400$. Parameters ε_+ and ε_- were varied between 0 and 0.01. Initial values were $M_B[i](0) = 100$, $M_{AB}[i](0) = 0$ and $M_A[i](0) = 0$, while $M_A[1](t)$ was held at 100 in each time step. The last condition ensures the continuous influx of A particles into the reaction space. The process was simulated over 60,000 time steps.

Results and discussions

Fig. 1 shows two Liesegang patterns formed in the presence and absence of external electric field. It can be clearly seen that migration of the outer electrolyte is faster in case of a ''positive field'' than in the absence of any external agitation. Therefore the distance of the last band measured from the gel surface increases.

The thickness of the zones decreases when the strength of the external field is increased. The width law for various field strengths is shown in Fig. 2. The results suggest that the width law $w_n \propto X_n^\alpha$ still holds, but in an electric field α decreases monotonically with the increasing field strength. The precise values are given in Table 1.

We investigated the time law, as well. As Fig. 3 shows, in the absence of any external electric field propagation of the reaction front follows purely diffusive kinetics ($X_n \propto t_n^{1/2}$, continuous line).

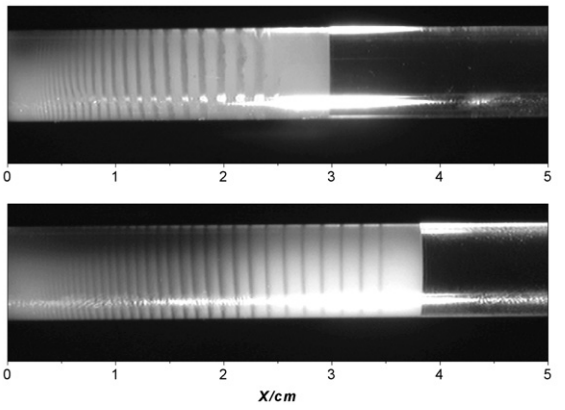

Fig. 1 Precipitate patterns in the absence (top) and in the presence of an electric field ($\mathbf{E} = 12$ V m^{-1}, bottom). Evolution time was 40.82 h in both cases. Black stripes represent solid precipitate, while the white areas correspond to colloidal distribution of reaction product.

According to some real experiments[24,27,28,30] and deterministic simulations[30,32] performed by other authors in the case with an electric field we expect that the band position shows a quadratic dependence on the square root of time. The amplitude of band fluctuations decreases both in space and time as the field strength increases. The effect of random fluctuations becomes relatively small in the high field region, because the probability distribution of elementary particle movements becomes more and more asymmetric.

The effect of the external field on the zone thickness has been investigated, as well. The results are summarized on Fig. 4. Values belonging to the first and last two bands were omitted. The simulation results exhibit considerable uncertainty. Table 2 shows the values of the exponent α for some different cases. It is interesting to note that in the field free case the results do not coincide with the experimental ones (Table 1 and refs. 12–14) nor with the results of the deterministic model.[17] All of these proposed that α should fall very close to unity. We guess that this marked difference is caused by the relatively small number

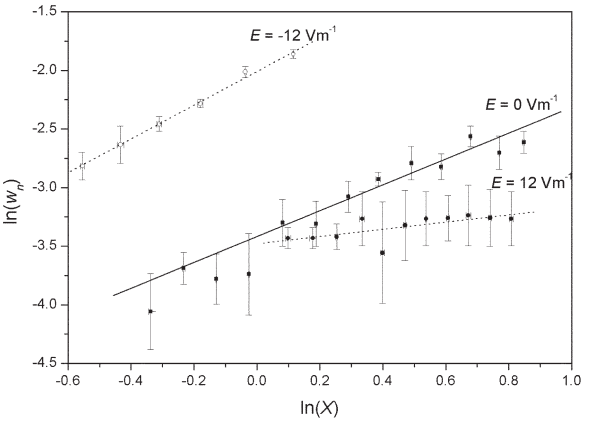

Fig. 2 Connection of zone thickness and position for various field strengths (real experiments). The solid line represents the field free case.

Table 1 Variation of the exponent α of the width law with electric field strength in real experiments

$\mathbf{E}$/V m^{-1}	α
18.0	0.165
12.0	0.307
0	1.104
−12.0	1.458

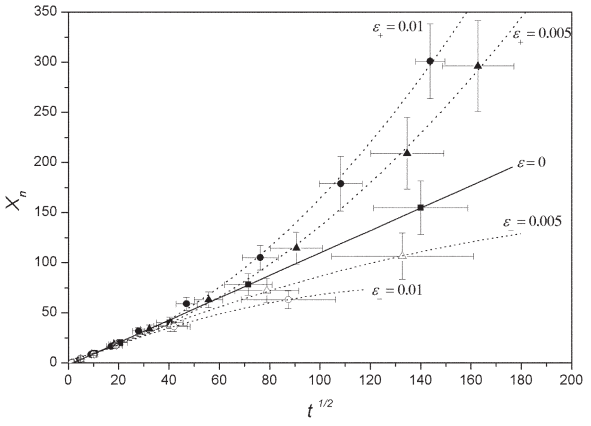

Fig. 3 Evolution curves of Liesegang patterns in stochastic simulations. All points represent the average of 30 runs, and correspond to the distance of a precipitate zone measured from the beginning of the reaction medium. The solid line corresponds to the field free case, the dotted ones represent the patterns formed in fields with various strengths. The error bars correspond to the 95% confidence level.

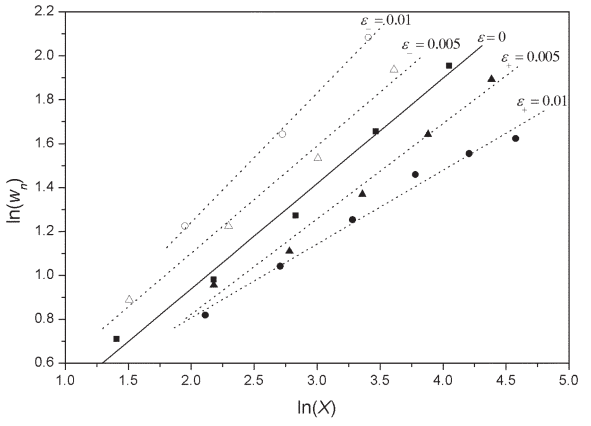

Fig. 4 Connection of zone thickness and position for various field strengths (stochastic simulations). Every point represents the average of 30 different runs.

Table 2 Variation of the exponent α of the width law with electric field strength; results of stochastic simulations

Electric field strength	α
$\varepsilon_+ = 0.01$	0.336
$\varepsilon_+ = 0.005$	0.435
$\varepsilon = 0$	0.480
$\varepsilon_- = 0.005$	0.489
$\varepsilon_- = 0.01$	0.590

of particles. At the same time change of α with the field strength shows very similar behavior in experiments and simulations. α decreases with increasing field strength in both cases.

Table 3 shows the spacing coefficient (P_{sp}) determined from the simulations, as a function of the electric field strength. It was found that the spacing coefficient decreases with increasing field strength just like in the real experiments.[30] Although we have obtained higher values for this parameter than observed in reality[30] and found in deterministic simulations,[30] the trend of the change has been successfully reproduced. (The spacing coefficient of the real Liesegang patterns usually falls between 1.04 and 1.4.)

Fig. 5 shows the spatial distribution of the precipitate for various electric field strengths.

Table 3 Variation of the spacing coefficient (P_{sp}) with electric field strength (simulations)

Electric field strength	P_{sp}
$\varepsilon_+ = 0.01$	1.682
$\varepsilon_+ = 0.005$	1.803
$\varepsilon = 0$	1.899
$\varepsilon_- = 0.005$	1.905
$\varepsilon_- = 0.01$	2.111

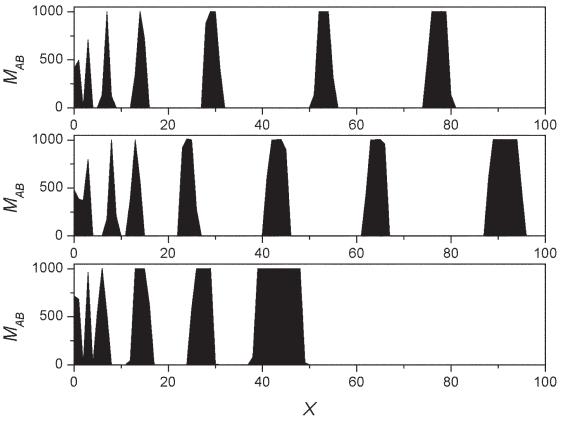

Fig. 5 Spatial distribution of the precipitate at various electric field strengths: $\varepsilon_+ = 0.01$ (top), $\varepsilon = 0$ (middle) and $\varepsilon_- = 001$ (bottom) in a single simulation.

Conclusions

The study presented here focused on the stochastic simulation of Liesegang patterns in an external electric field. Our intention was twofold. First, we wanted to see whether this new theoretical approach can reproduce our own experimental results, and those published recently in the literature.[24,27,28,30] Second, we tried to explore the main features of Liesegang patterning, when it is combined with an external field.

Our results can be summarized as follows. In the presence of an electric field the position of bands, measured from the junction point of electrolytes can be characterized by the function $X_n = a(\varepsilon)t^{1/2} + b(\varepsilon)t + c(\varepsilon)$, where $a(\varepsilon)$, $b(\varepsilon)$ and $c(\varepsilon)$ are parameters depending on electric field strength. Taking the limit $\varepsilon_+ \to 0$ or $\varepsilon_- \to 0$, results in $a(\varepsilon) \to a_o$, $b(\varepsilon) \to 0$ and $c(\varepsilon) \to c_o$.

In a former paper[30] we have shown both by simulations and real experiments that the spacing coefficient, that describes the overall structure of a Liesegang pattern decreases with increasing field strength. Results of the present stochastic approach coincide with this earlier finding.

Finally, we have proposed an extended form of the width law, which takes into account the effect of constant electric field. The general form of this scaling law is $w_n \propto X_n^{\alpha(\varepsilon)}$, where $\alpha(\varepsilon)$ is a decreasing function of its argument. Again this result is in good agreement with the experimental observations.

All these results show that the stochastic approach presented here is an effective method to simulate the formation and dynamics of Liesegang patterns even in an external electric field.

Acknowledgements

We thank Drs A. Büki and T. Turányi for helpful discussions and Drs Á. Tóth and D. Horváth for their contribution to the experimental work. The experiments were carried out at the Department of Physical Chemistry of University of Szeged.

The authors acknowledge the support of OTKA grant F034840.

References

1 R. E. Liesegang, *Naturwiss. Wochenschr.*, 1896, **11**, 353.
2 G. Venzl and J. Ross, *J. Chem. Phys.*, 1982, **77**, 1302.
3 M. E. LeVan and J. Ross, *J. Phys. Chem.*, 1987, **91**, 6300.
4 A. A. Polezhaev and S. C. Müller, *Chaos*, 1994, **4**, 631.
5 A. Büki, É. Kárpáti-Smidróczki and M. Zrinyi, *J. Chem. Phys.*, 1995, **103**, 10 387.
6 H.-J. Krug and H. Brandtstädter, *J. Phys. Chem. A*, 1999, **103**, 7811.
7 T. Antal, M. Droz, J. Magnin and Z. Rácz, *Phys. Rev. Lett.*, 1999, **83**, 2880.
8 Z. Rácz, *Physica A*, 1999, **274**, 50.
9 M. Al-Ghoul and R. Sultan, *J. Phys. Chem. A*, 2001, **105**, 8053.
10 K. Jablczynski, *Bull. Soc. Chim. Fr.*, 1923, **33**, 1592.
11 H. W. Morse and G. W. Pierce, *Proc. Am. Acad. Arts Sci.*, 1903, **38**, 625.
12 K. M. Pillai, V. K. Vaidyan and M. A. Ittyachan, *Colloid Polym. Sci.*, 1980, **258**, 831.
13 S. C. Müller, S. Kai and J. Ross, *J. Phys. Chem.*, 1982, **86**, 4078.
14 M. Droz, J. Magnin and M. Zrinyi, *J. Chem. Phys.*, 1999, **110**, 9618.
15 R. Matalon and A. Packter, *J. Colloid Sci.*, 1955, **10**, 46.
16 T. Antal, M. Droz, J. Magnin, Z. Rácz and M. Zrinyi, *J. Chem. Phys.*, 1998, **109**, 9479.
17 G. T. Dee, *Phys. Rev. Lett.*, 1986, **57**, 275.
18 B. Chopard, P. Luthi and M. Droz, *Phys. Rev. Lett.*, 1994, **72**, 1384.
19 B. Chopard, P. Luthi and M. Droz, *J. Stat. Phys.*, 1994, **76**, 661.
20 F. Izsák and I. Lagzi, *Chem. Phys. Lett.*, 2003, **371**, 321.
21 P. Happel, R. E. Liesegang and O. Mastbaum, *Kolloid Z.*, 1929, **48**, 80.
22 B. Kisch, *Kolloid Z.*, 1929, **49**, 154.
23 P. Happel, R. E. Liesegang and O. Mastbaum, *Kolloid Z.*, 1929, **48**, 252.
24 A. H. Sharbaugh III and A. H. Sharbaugh, *J. Chem. Educ.*, 1989, **66**, 589.
25 I. Das, A. Pushkarna and A. Bhattacharjee, *J. Phys. Chem.*, 1990, **94**, 8968.
26 I. Das, A. Pushkarna and A. Bhattacharjee, *J. Phys. Chem.*, 1991, **95**, 3866.
27 R. Sultan and R. Halabieh, *Chem. Phys. Lett.*, 2000, **332**, 331.
28 R. F. Sultan, *Phys. Chem. Chem. Phys.*, 2002, **4**, 1253.
29 R. Sultan and S. Panjarian, *Physica D*, 2001, **157**, 241.
30 I. Lagzi, *Phys. Chem. Chem. Phys.*, 2002, **4**, 1268.
31 W. Ostwald, *Kolloid Z.*, 1925, **36**, 380.
32 M. Al-Ghoul and R. Sultan, *J. Phys. Chem. A*, 2003, **107**, 1095.
33 S. Kai, S. C. Müller and J. Ross, *J. Phys. Chem.*, 1983, **87**, 806.
34 S. Kai and S. C. Müller, *Sci. Form*, 1985, **1**, 9.
35 T. Antal, M. Droz, J. Magnin, A. Pekalski and Z. Rácz, *J. Chem. Phys.*, 2001, **114**, 3770.
36 A. Büki, É. Kárpáti-Smidróczki and M. Zrinyi, *Physica A*, 1995, **220**, 357.